The Plant Journal (2004) **38**, 923–939 doi: 10.1111/j.1365-313X.2004.02094.x

The *Etched1* gene of *Zea mays* (L.) encodes a zinc ribbon protein that belongs to the transcriptionally active chromosome (TAC) of plastids and is similar to the transcription factor TFIIS

Oswaldo da Costa e Silva[1,†,‡], René Lorbiecke[1,‡], Preeti Garg[1], Lenard Müller[2], Martina Waßmann[1], Patricia Lauert[1], Mike Scanlon[3], An-Ping Hsia[4], Patrick S. Schnable[4], Karin Krupinska[2] and Udo Wienand[1,*]

[1]*Institut für Allgemeine Botanik und Botanischer Garten, Universität Hamburg, Ohnhorststr. 18, D-22 609 Hamburg, Germany,*

[2]*Botanisches Institut der Christian-Albrechts-Universität zu Kiel, Olshausenstr. 40, 24098 Kiel, Germany,*

[3]*University Georgia, 3609 Plant Sciences, Athens, GA 30602, USA, and*

[4]*Department of Agronomy and Center for Plant Genomics, Iowa State University, Ames, IA 50011, USA*

Received 25 November 2003; revised 20 February 2004; accepted 2 March 2004.

*For correspondence (fax +49 40 42816503; e-mail udo.wien@uni-hamburg.de).

†Present address: BASF Plant Science GmbH, BPS-A30, 67056 Ludwigshafen, Germany.

‡Both authors contributed equally to this paper.

Summary

***Etched1* (*et1*) is a pleiotropic, recessive mutation of maize that causes fissured and cracked mature kernels and virescent seedlings. Microscopic examinations of the *et1* phenotype revealed an aberrant plastid development in mutant kernels and mutant leaves. Here, we report on the cloning of the *et1* gene by transposon tagging, the localization of the gene product in chloroplasts, and its putative function in the plastid transcriptional apparatus. Several alleles of *Mutator* (*Mu*)-induced *et1* mutants, the *et1-reference* (*et1-R*) mutant, and *Et1* wild-type were cloned and analyzed at the molecular level. Northern analyses with wild-type plants revealed that *Et1* transcripts are present in kernels, leaves, and other types of tissue, and no *Et1* expression could be detected in the *et1* mutants analyzed. The ET1 protein is imported by chloroplasts and has been immunologically detected in transcriptionally active chromosome (TAC) fractions derived from chloroplasts. Accordingly, the relative transcriptional activity of TAC fractions was significantly reduced in chloroplasts of *et1-R* plants. ET1 is the first zinc ribbon (ZR) protein shown to be targeted to plastids. With regard to its localization and its striking structural similarity to the eukaryotic transcription elongation factor TFIIS, it is feasible that ET1 functions in plastid transcription elongation by reactivation of arrested RNA polymerases.**

Keywords: etched1, plastid nucleoids, transcriptional active chromosome, transposon tagging, plastid transcription, TFIIS.

Introduction

The analysis of genes involved in the development of the maize endosperm is of particular interest in order to understand the structural and regulatory features of seed growth. In maize, many mutants and a number of genes affecting tissue and organ development have been isolated. Numerous mutants have been described, which exhibit abnormal endosperm development (for review: Coe *et al.*, 1988). Among these, a few are pleiotropic and thus of particular interest because they affect the development of different tissue types. *Etched1* (*et1*) is one such mutation, which affects the development of kernels as well as of seedlings.

Etched1 is a recessive mutation that was first identified and described by Stadler (1940). The mutant reference allele (*et1-reference* (*et1-R*)) was isolated from the progeny of a population of maize plants pollinated with X-ray irradiated pollen. Kernels homozygous for the *et1-R* allele are fissured because of depressions and crevices on the endosperm surface (Figure 1a–c). Prior biochemical and

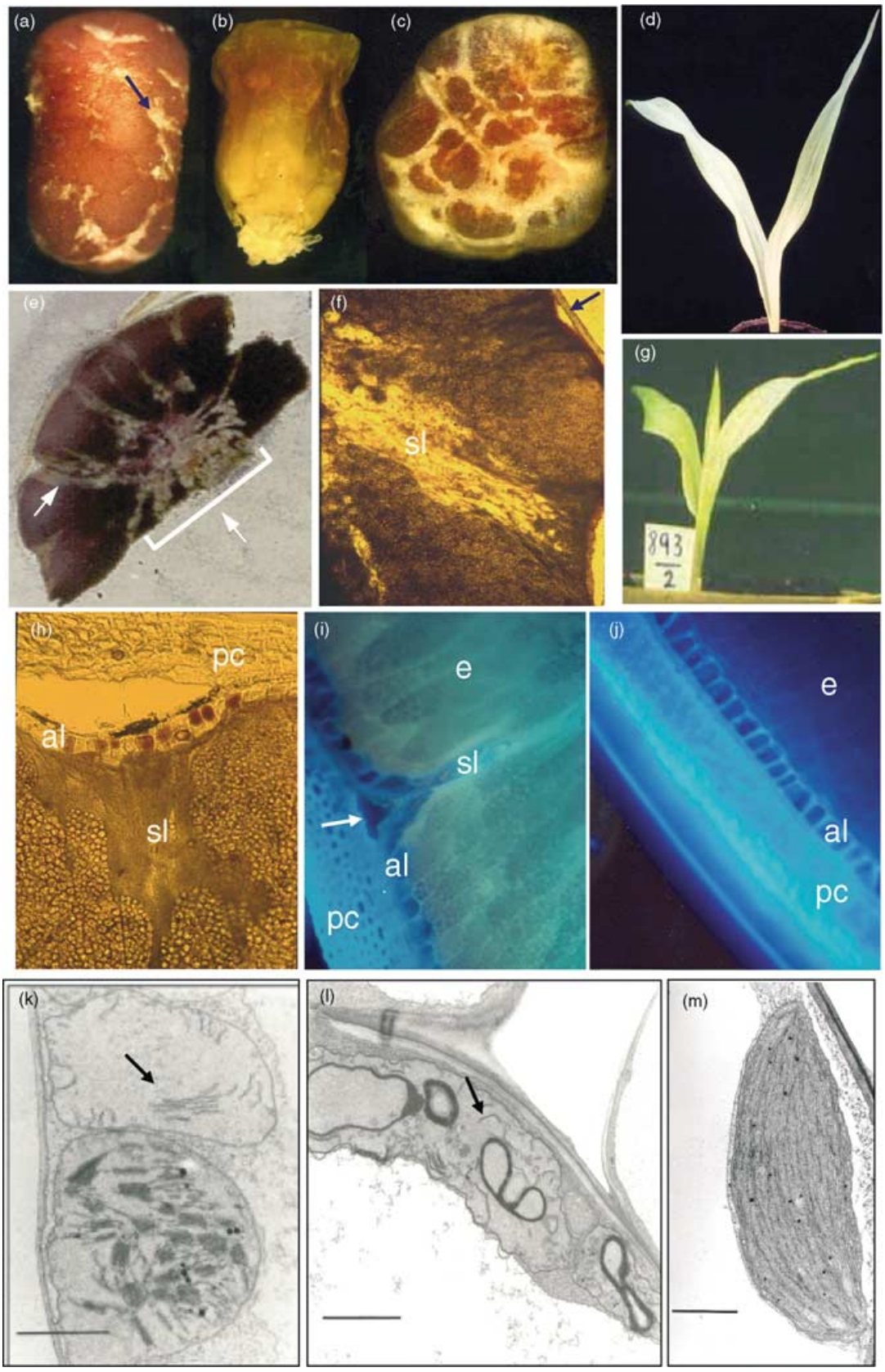
(a)
(b)
(c)
(d)
(e)
(f)
sl
(g)
893
2
(h)
pc
al
sl
(i)
e
sl
al
pc
(j)
e
al
pc
(k)
(l)
(m)

structural analyses of the *et1-R* kernels revealed that starch synthesis is reduced and starchless endosperm cells are present around the cracks and scars in the kernels (Figure 1; Sangeetha and Reddy, 1991). The *et1* kernel phenotype becomes visible approximately 15 days after pollination (DAP). The degree of etching differs among the kernels on an ear and can vary from a weak to a very severe phenotype. This phenotypic variation is apparently not correlated with any specific genetic background (Sangeetha and Reddy, 1991).

et1 mutant seedlings exhibit a virescent phenotype, i.e. their leaves are initially pale green (Figure 1d,g) but become fully green approximately 2 weeks after germination. The effect of the *et1* mutation on seedling growth primarily concerns chloroplast development. During initial leaf growth, the morphogenesis of chloroplasts in mutant seedlings is impaired or delayed (Figure 1k–m). Carotenoids, chlorophyll pigments, and chlorophyll–protein complexes accumulate at reduced levels in the *et1* leaves (Ramesh *et al.*, 1984; Sangeetha *et al.*, 1986). However, after approximately 2 weeks, a shift to normal chloroplast development occurs and the yellow to pale-green leaves turn fully green. Further growth and development of the plant is normal and does not appear to be influenced by the mutation (Sangeetha and Reddy, 1991). This suggests that the ET1 protein is required for a fundamental process during plastid differentiation early in seedling and kernel development.

Additional *et1* mutants (*et1-M*) have been isolated from active *Mutator* (*Mu*) lines (Scanlon *et al.*, 1994; this report). Among these mutants, some exhibit a phenotype distinct from that of the *et1-R* plants. The homozygous kernels for these *et1* alleles are shrunken, severely etched, and develop either no or only small embryos. These differences in phenotypes appear to be the result of allelic differences among the mutants. Scanlon *et al.* (1994) have shown that crosses of these *et1-M* mutants with the reference allele weaken the severe phenotype in an allele dosage-dependent manner.

In this report, we describe the isolation and characterization of the *Et1* gene using a forward gene-tagging approach. We further report on the identification of the ET1 protein as part of the transcriptionally active chromosome (TAC) derived from plastid nucleoids (Hallick *et al.*, 1976; Krause and Krupinska, 2000; Suck *et al.*, 1996). The sequence of the ET1 protein exhibits significant similarity to the zinc ribbon (ZR) domain of the eukaryotic transcription factor TFIIS. TFIIS (also known as SII) is capable of reactivating arrested RNA polymerase II (Pol II) by inducing the intrinsic ribonuclease activity of the polymerase. After removal of displaced nucleotides at the 3′ end of the nascent RNA, polymerization is re-started (Kettenberger *et al.*, 2003; Opalka *et al.*, 2003).

ET1 is the first identified member of a new family of plastid localized ZR proteins. Based on our data, we hypothesize that the ET1 protein plays a role in transcript elongation in chloroplasts similar to the role of TFIIS in RNA Pol II transcription. This function is in agreement with the retarded chloroplast development observed in leaves of the *et1* mutant.

Results

Isolation of the et1 *gene from the* Mu*-induced allele,* et1-M3

Several *Mu*-induced *et1* mutants were used for the isolation of the gene locus by a transposon-tagging strategy (review: Chomet, 1994; Wienand *et al.*, 1982). Cloning of the *et1* gene was conducted using *et1-M3*, one of the *Mu* transposon-induced mutant alleles available (Scanlon *et al.*, 1994). A modified amplification of insertion mutagenized sites (AIMS) procedure (Frey *et al.*, 1998; Lauert *et al.*, 1999) was used to identify and isolate genomic fragments that co-segregated with the etched phenotype. A 171-bp *Hpa*II/G PCR fragment was identified from populations segregating for mutant (*et1-R/et1-M3*) and wild-type (*et1-R/Et1*) phenotypes (AIMS-1; Figure 2). This fragment could only be amplified from genomic DNA isolated from mutant plants (21 individuals analyzed) and was not detectable in wild-type plants (15 individuals analyzed). In a more detailed AIMS analysis using this mutant, two further PCR fragments, an 83-bp *Mse*I/C and a 157-bp *Hin*PI/G fragment (AIMS-2 and

Figure 1. *etched1* phenotype.
(a–c) Stereomicroscopic view of mature, desiccated kernels homozygous for *et1-R*, *et1-M3*, and *et1-M16,* respectively. The fissures observed on the kernel surface are a characteristic phenotype of *et1* mutants (blue arrow).
(d, g) Virescent seedlings of *et1-M15*/*et1-R* and *et1-R* genotypes, respectively.
(e, f) Thin transverse hand sections of 20 DAP *et1-R* kernels. (e) Transverse section stained with IKI. The starchy endosperm cells are colored deep violet. Starchless cells can be observed as colorless regions radiating out from the center up to the periphery (white arrows). (f) Enlarged stereo-microscopic view (5×) of the endosperm showing starchless (sl) sectors and a depression (blue arrow).
(h) Enlarged stereo-microscopic view (20×) of the peripheral region of an sl sector. Note the typical surface depression and a colored and intact aleurone (al) layer, which is pulled away from the multilayered pericarp (pc).
(i) Longitudinal cross-section of a mature, desiccated *et1-M3*/*et1*-R kernel photographed under UV-epifluorescent light. The arrow points to a fissure as shown in (a) and (h). Note the presence of intact al cells and collapsed walls of the sl endosperm cells beneath the fissure (e = endosperm).
(j) Longitudinal cross-section of a mature, desiccated LC (wild type) kernel photographed under UV-epifluorescent light. Note the well-structured al layer and e tissue.
(k, l) Ultrastructure of *et1-M3*/*et1*-R chloroplasts. Sections were prepared from leaves of virescent seedlings. Note the lack of organized thylakoid and grana structures (arrows).
(m) Ultrastructure of a wild-type chloroplast isolated from LC with highly organized thylakoid structures (bars = 1 μm).

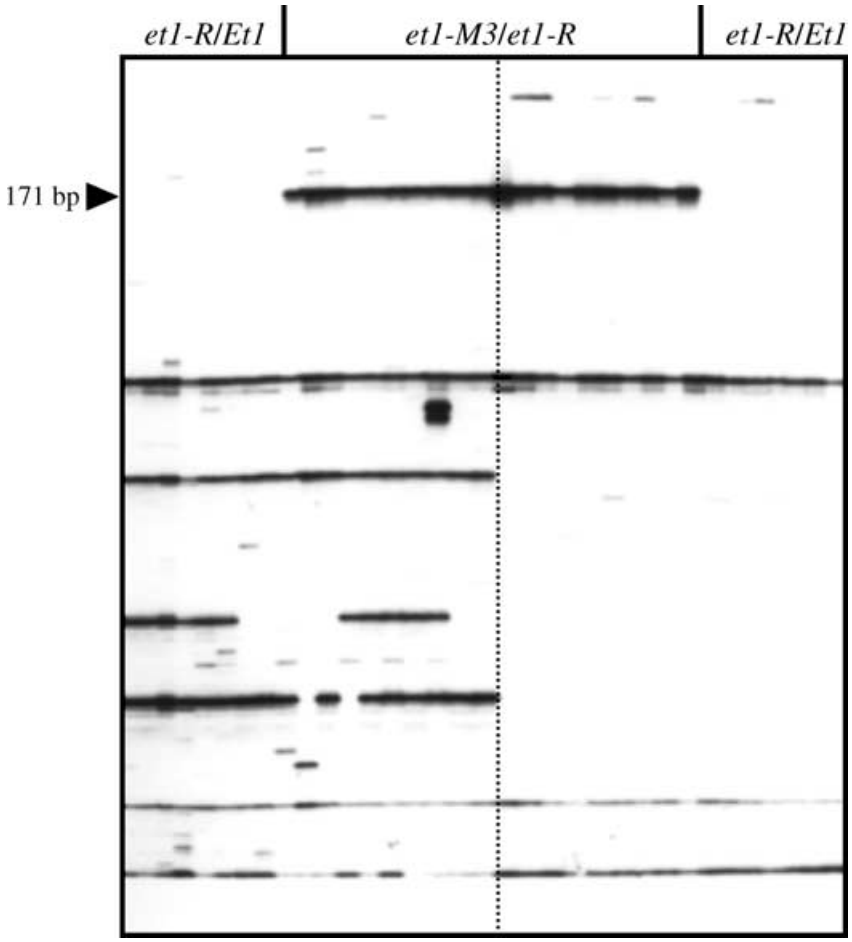

Figure 2. AIMS mapping of the transposon insertion site in the *et1-M3* allele.
AIMS analysis with maize genomic DNA amplified with the *Hpa*II/G enzyme-select primer. Genotypes of the different individuals analyzed are indicated on top. Equal number of siblings from two different populations were used, both segregating for plants either carrying the *et1-M3* mutation (*et1-R/et1-M3*) or possessing a wild-type phenotype (*et1-R/Et1*). A 171-bp fragment (arrowhead; AIMS-1 in Figure 3) co-segregated with the *et1-M3* mutant plants (*et1-M3/et1-R*).

AIMS-3, Figure 3a), were identified to co-segregate with the *et1-M* phenotype.

The 171-bp *Hpa*II/G fragment was used to isolate putative *Et1* genomic clones from a lambda library derived from plants with a heterozygous *et1-M3/Et1-B73* genotype, from which clones representing wild-type (*Et1*) or mutant alleles (*et1*) could be expected. Four different clones were isolated from this screen. One of them, λ*et1-M3*-c5, that contains a *Mu8* element insert (Figure 3a) represents the mutant allele. Two other clones, λ*Et1*-c11 and λ*Et1*-c14 that lack *Mu* insertions, represent wild-type allele *Et1-B73* (Figure 3b). A 2.5-kbp *Hin*dIII/*Xho*I fragment (Frag 3 in Figure 3b) from clone λ*Et1*-c11 was used for RFLP mapping. This clone mapped to the long arm of chromosome 3 (3.09), between markers *cdo962B* and *npi425A*, i.e. approximately to the same position to which the *et1* gene has been mapped (Neuffer *et al.*, 1997).

Analysis of additional et1 *mutant alleles*

Further evidence of having cloned the *Et1* gene came from the analysis of additional *et1-M* alleles as well as of the reference allele *et1-R*. Single-copy sequences from clones λ*et1*-c11 and λ*et1*-c14 were used to clone and isolate corresponding sequences from the mutant alleles *et1-M12* (provided by P. Stinard), *et1-M15*, and *et1-M16* (both isolated by a directed tagging approach). The sequence of *et1-M10* (Scanlon *et al.*, 1994) was isolated via PCR amplification experiments.

A detailed analysis of the *et1* locus from these *et1-M* mutants revealed a *Mu* insertion in all these alleles, either at the same position or in the vicinity of the *Mu8* insertion found in *et1-M3* (Figure 4a). Hybridization analysis of the *et1-R* genomic clone using different wild-type genomic fragments as probes revealed deletions and rearrangements around the locus (Figure 3c,d). In contrast to the mutant, wild-type alleles from the inbred genotypes Line C (LC) and B73 (the progenitor of *et1-M3*) contain no *Mu* element insertions in the corresponding sequences. These analyses strongly indicated that the cloned sequences represent the *et1* locus.

Sequence analysis of Et1 *and* et1 *alleles*

The *Et1* sequences from wild-type clones mentioned above were used to isolate a full-length *Et1* cDNA (c*Et1*-9) from a

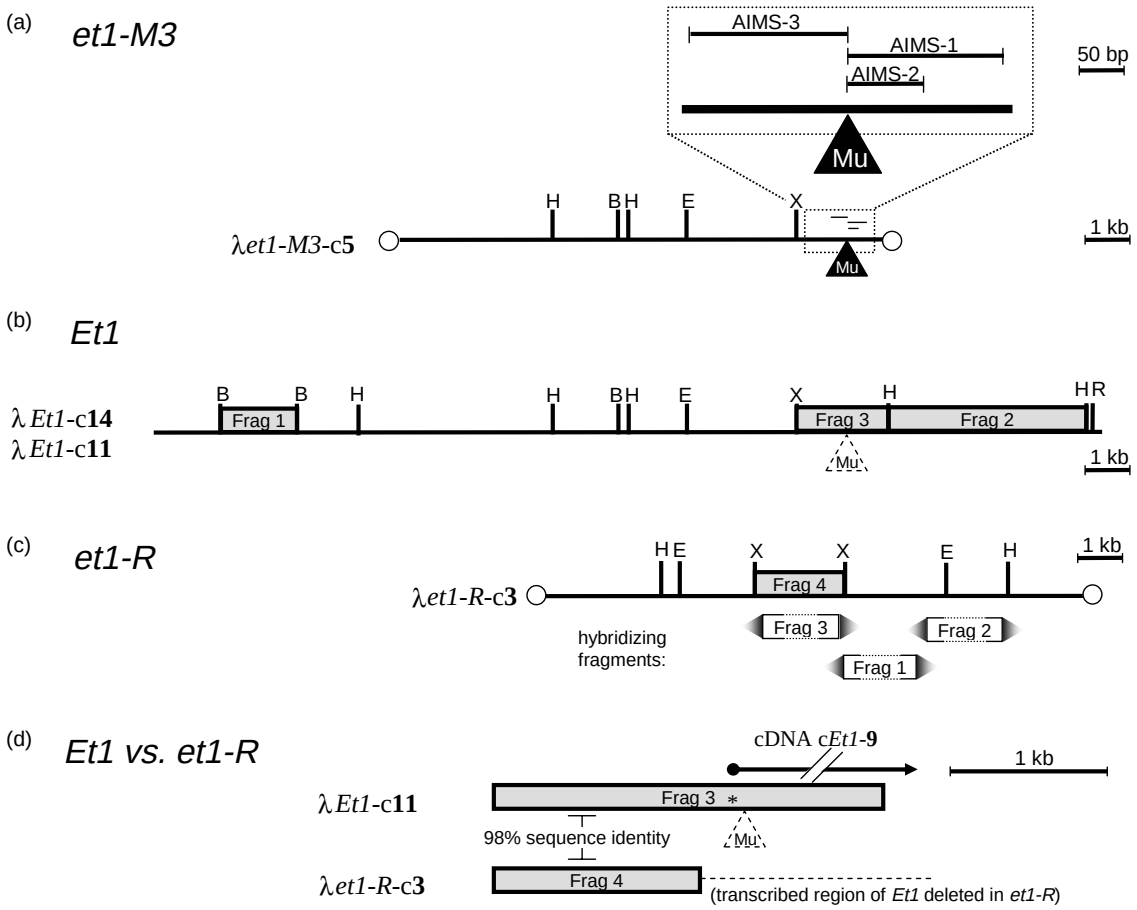

Figure 3. The *et1* genomic locus and a comparison between the wild-type, *et1-M3*, and *et1-R* alleles.
(a) Restriction enzyme map of the *et1-M3* mutant genomic λ-clone *et1-M3*-c5. The position of a *Mu8* element insertion at the *et1* locus is shown as a filled triangle. This region is shown enlarged above the clone with the positions of the isolated AIMS fragments (which co-segregated with the *et1-M3* mutation) relative to the position of the *Mu8* insertion (AIMS-1: 171-bp *Hpa*II/G fragment (Figure 2); AIMS-2: 83-bp *Mse*I/C fragment; and AIMS-3: 157-bp *Hin*PII/G fragment).
(b) Restriction enzyme map based on two *Et1* wild-type genomic λ-clones, *Et1*-c14 and *Et1*-c11. For comparison, the position of the *Mu8* element insertion in the *et1-M3* mutant allele (see a) is shown as a dashed triangle. Subfragments of the two wild-type clones (Frag 1–Frag 3) were used for further hybridization experiments (description below).
(c) Restriction enzyme map of the *et1-R* genomic λ-clone *et1-R*-c3. The regions hybridizing with wild-type *Et1* probes Frag 1–Frag 3 are shown as open rectangles. The dotted lines symbolize that the exact location is not known.
(d) Schematic comparison between the sequences derived from *Et1* Frag 3 and *et1-R* Frag 4. Note that the sequence identity does not encompass the transcribed region of the *Et1* gene. The (*) marks the position of the first nucleotide of the cDNA clone c*Et1*-9. A dashed triangle indicates the location of the *Mu*8 insertion in the *et1-M3* mutant allele.
The open circles in (a,c) represent the arms of the lambda vector. B, *Bam*HI; H, *Hin*dIII; E, *Eco*RI; and X, *Xho*I.

lambda cDNA library prepared from wild-type LC-developing kernels 13–28 DAP. This cDNA is 772 bp in length and contains an open-reading frame (ORF) of 163 amino acids (aa; Figure 4a). The structure of the gene was elucidated by comparison of this cDNA sequence to wild-type genomic clones. The *Et1* gene contains four exons of length 164, 88, 129, and 281 bp, and three introns of length 75, 670, and 145 bp (data not shown).

By comparison of wild-type *Et1* gene structure with the *et1-M* mutant alleles analyzed, the positions of the *Mu* element insertions were identified. In the alleles *et1-M3*, *et1-M10*, *et1-M12*, and *et1-M15*, a *Mu8* element was present in the 5′ untranslated region (UTR) of the *et1* gene. Interestingly, the position of insertion and orientation of the *Mu* element was identical for *et1-M10* and *et1-M12* (in 5′ to 3′ orientation), as well as for *et1-M3* and *et1-M15* (in 3′ to 5′ orientation). This is not rather surprising as independent Mu-insertion sites at identical positions have also been described for *glossy* and *bronze* genes (Dietrich *et al.*, 2002). Moreover, these two positions of insertion were in close proximity to each other (Figure 4a).

In the case of the *et1-M16* allele, a *Mu1* element was present in the first exon within the ORF in 5′ to 3′ orientation. In the case of *et1-R*, nearly the complete *et1* gene was

(a)

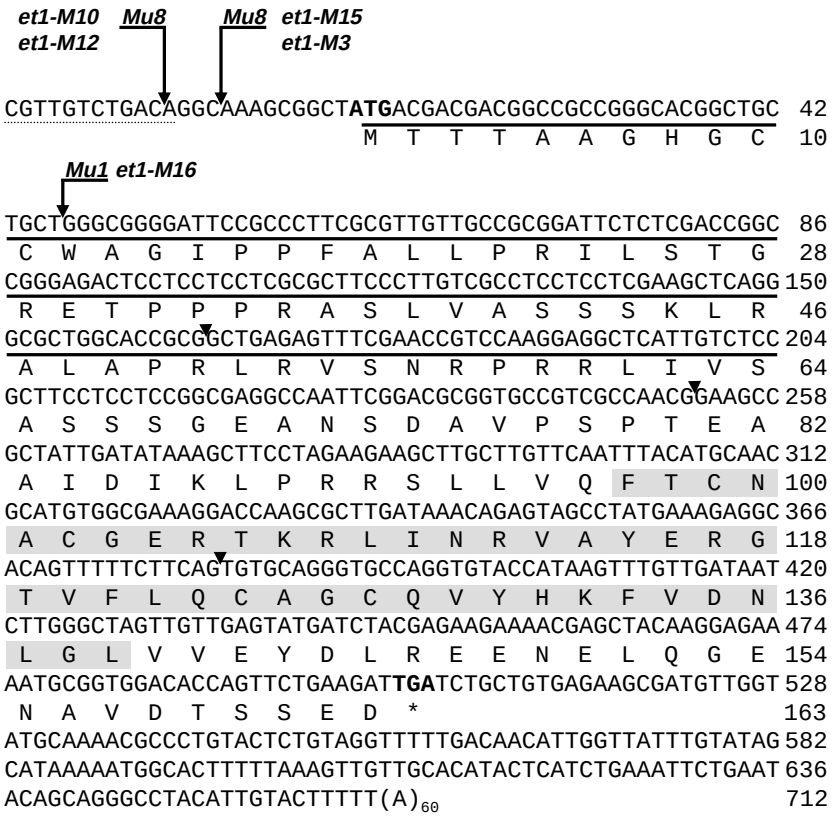

(b)

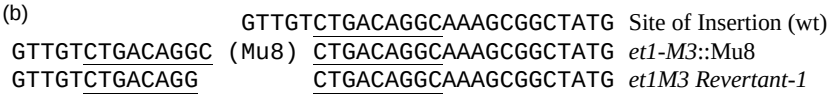

Figure 4. Sequence analysis of the *et1* gene of maize.
(a) *Et1* cDNA sequence and its deduced amino acid sequence. The positions of the *Mu* insertions in the different *et1-M* alleles are depicted with arrows. The lengths in nucleotides for the cDNA sequence (beginning with the first nucleotide of the cDNA c*Et1*-9) and amino acids for the protein sequence are shown on the right of the two sequences. The dotted line at the beginning of the nucleotide sequence shows the *et1* genomic sequence upstream of the cloned cDNA sequence. A poly(A) tail of 60 residues was present at the 3′ end of this cDNA clone. The arrowheads along the nucleotide sequence represent the positions of introns in the genomic sequence. The start and stop codons are written in bold. The amino acids are presented in one-letter codes below the corresponding codons. The putative N-terminal plastid transit sequence is underlined. The residues constituting the ZR domain are shaded gray. The stop codon is represented as (*).
(b) *Mu8* insertion site in the *et1-M3* mutant allele and sequence of a somatic revertant of *et1-M3*. The basepairs that are duplicated because of *Mu8* insertion are underlined and compared to wild-type *Et1* gene. One single nucleotide of the 9-bp duplication is missing upon *Mu8* excision in the *et1-M3* revertant (footprint).

found to be deleted (Figure 3d), which is consistent with the finding that X-ray treatment usually causes DNA deletions.

To further prove the correct cloning of the *et1* gene, a green revertant sector of a young and otherwise pale *et1-M3* seedling leaf was analyzed via PCR experiments. These experiments revealed that in the revertant sector, the *Mu8* element was absent from its position of insertion in the *et1-M3* allele. However, an imperfect target-site duplication, typically left behind by transposons after excision, was observed (Figure 4b). As this *Mu8* element was present in the 5′ UTR of the gene, the transposon's excision footprint did not disturb the ORF, resulting in normal chloroplast development and wild-type phenotype in the revertant sector of the seedling leaf.

Expression of the Et1 *gene*

Northern experiments were performed with total RNA from different tissue types of wild-type as well as of mutant plants using the 3′ UTR of the *Et1* gene as a probe. No *Et1* expression was observed in any of the analyzed *et1* mutants (Figure 5a,b). The hybridizing mRNA observed in wild-type plants corresponded to a transcript length of approximately 750 nucleotides, as expected from the length of the cloned cDNA (Figure 4). The strongest hybridization signals were observed with RNAs from leaves at different stages of development, and from developing kernels (Figure 5a). In other parts of the plant, e.g. stems and silks, lower amounts of *Et1*-hybridizing mRNA accumulated (data not shown). After separating the embryo from 20 DAP kernels, *Et1* mRNA was almost exclusively detected in the remaining kernel tissue and not in the embryos (data not shown). This indicates that in the wild type, *Et1* is predominantly expressed in those types of tissue that exhibit the *et1* phenotype in the mutants.

To determine whether the expression of *Et1* in leaves is stimulated by light, RNA isolated from dark-grown etiolated wild-type seedlings was used for Northern analysis. These plants had a highly reduced *Et1* expression when compared to seedlings grown under normal light conditions (Figure 5b), indicating that light is a factor triggering *Et1* expression in this tissue.

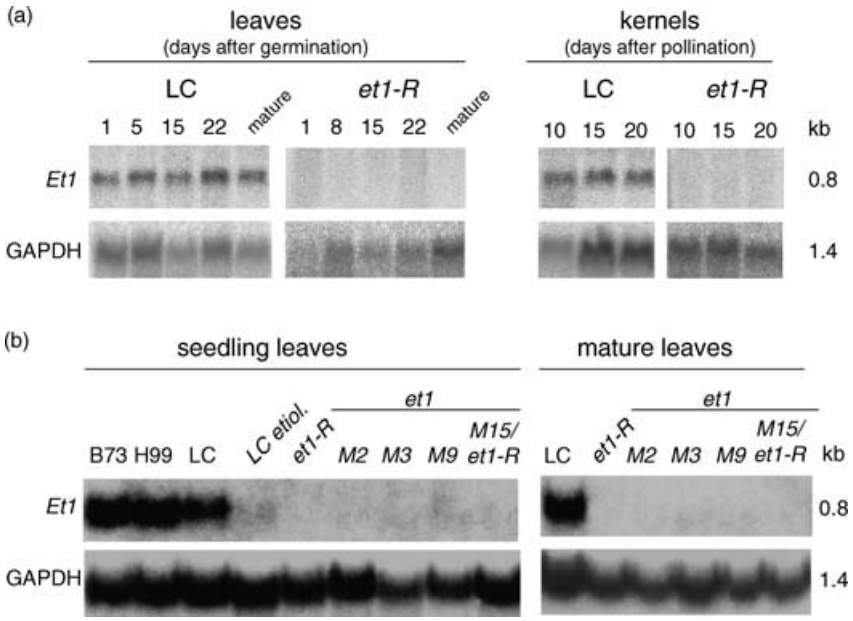

Figure 5. Expression pattern of the *et1* gene.
(a) Hybridization pattern of *Et1* cDNA to total RNA from wild-type and *et1-R* leaves and kernels at different stages of development. The number at the top of each subcolumn denotes the age of seedlings in days after germination or the age of kernels in DAP.
(b) Hybridization pattern of *Et1* cDNA to total RNA from seedling and mature leaves of various *et1* mutants and wild-type genotypes B73, H99, and LC. The mutants include *et1-R*, *et1-M2*, *et1-M3*, *et1-M9*, and the hybrid *et1-M15/et1-R*. The sample labeled 'LC etiol.' refers to an RNA preparation from etiolated LC seedlings, germinated, and grown under continuous darkness.
In (a,b), the expression of GAPDH (glyceraldehyde 3-phosphate dehydrogenase) is given as a control for equal RNA loading.

ET1 protein structure

The putative ET1 protein is 163 aa in length and has a deduced molecular weight of 19.6 kDa. Computational analyses of the ET1 protein sequence predicted an N-terminal transit sequence for plastid import. After cleavage of the transit sequence, the predicted mature protein would contain 99 aa with a predicted molecular weight of 11.9 kDa (Figure 4a). Database searches revealed a significant sequence similarity of the mature ET1 protein to the ZR domain (domain III) of the eukaryotic transcription factor TFIIS (also known as SII) from yeast, fission yeast, and human (Figure 6a,b). The ET1 sequence has lower similarity to other ZR-containing proteins, e.g. RNA polymerase II subunit 9 (Rpb9) (Figure 6a; Hemming and Edwards, 2000; Wang *et al.*, 1998). Based on tertiary structure models of yeast TFIIS and the TFIIS/RNA Pol II complex, the ZR domain is characterized by a three-stranded β-sheet structure, possessing four cysteine residues, which are held together by a zinc atom and an acidic hairpin loop containing two invariant acidic residues, D and E, essential for TFIIS activity. The TFIIS ZR domain inserts deeply into the RNA Pol II pore and positions the two acidic residues in the enzyme's active site. In eukaryotes, TFIIS is essential for reactivating arrested RNA Pol II complexes. This is achieved by a conformational change in the active site of the enzyme that enhances the intrinsic ribonuclease activity. Ribonucleolytic cleavage of displaced 3′ ends of nascent RNA is required for progression of RNA polymerization (Awrey *et al.*, 1998; Conaway *et al.*, 2003; Kettenberger *et al.*, 2003 and citations therein; Opalka *et al.*, 2003 and citations therein). Thereby, TFIIS mitigates pausing of the RNA polymerase and increases the overall elongation rate.

Among the conserved amino acids shared between TFIIS and ET1 are four putative cysteine ligands of the zinc atom and one of the two acidic residues (aa E116; Figure 6a). The secondary structure of the ET1 protein was deduced using different *in silico* methods. Most of these methods predicted a three-stranded β-sheet structure strikingly similar to that of TFIIS. In addition, two α-helices in the interdomain linker and in the C-terminal region of domain II from TFIIS might also be conserved in ET1 (Figure 6a). Tertiary structure modeling of the ET1 ZR domain using the yeast TFIIS domain as template resulted in a comparable ZR structure for ET1 (Figure 6d). As is the case with residue E291 in TFIIS (Kettenberger *et al.*, 2003), the acidic residue E116 of ET1 is predicted to be exposed at the tip of the hairpin loop.

Furtheron, a number of non-annotated putative plant proteins with a high sequence similarity to ET1 were identified (Figure 6a,c). For none of these proteins a function has been assigned yet. The region of similarity is mainly restricted to the ZR domain. In maize, a very close ET1 homolog, *Zea mays* zinc ribbon 1 (ZmZR1; 87% similarity at the protein level) was cloned from the *et1-R* line (unpublished data). A phylogenetic analysis of ZR1 proteins showed two distinct subgroups for monocotyledonous and dicotyledonous plants, respectively. A putative ZR protein from the fern *Ceratopteris richardii* is more related to the dicotyledonous group (Figure 6c).

Computational analyses of the deduced ZmET1 and ZmZR1 proteins predicted N-terminal plastid target sequences for both (Figures 4 and 6b and data not shown). All other putative ZR1 plant proteins were also predicted to contain N-terminal plastid import sequences (data not shown).

The ET1 protein is imported into chloroplasts

To verify that ET1 is a plastid protein, chloroplast import experiments were conducted using *in vitro* translated and radioactively labeled ET1 protein and spinach chloroplasts. These experiments (Figure 7) showed that the ET1 protein is imported into the stroma of chloroplasts and that it contains an N-terminal transit peptide, which is cleaved off after transport, resulting in a reduced size of the mature protein in the stroma fraction. The size of the processed protein is in agreement with the prediction (Figure 4a). The absence of the ET1 protein from membrane fractions either treated with protease or untreated indicates that it is not associated with thylakoid membranes (Figure 7).

To determine if ET1 is imported into chloroplasts through the general import pathway (Soll and Tien, 1998), an unlabeled competitor protein, known to be transported through this pathway, was included in these experiments. With increasing amounts of the competitor protein, decreasing amounts of ET1 were detected in the chloroplast stroma

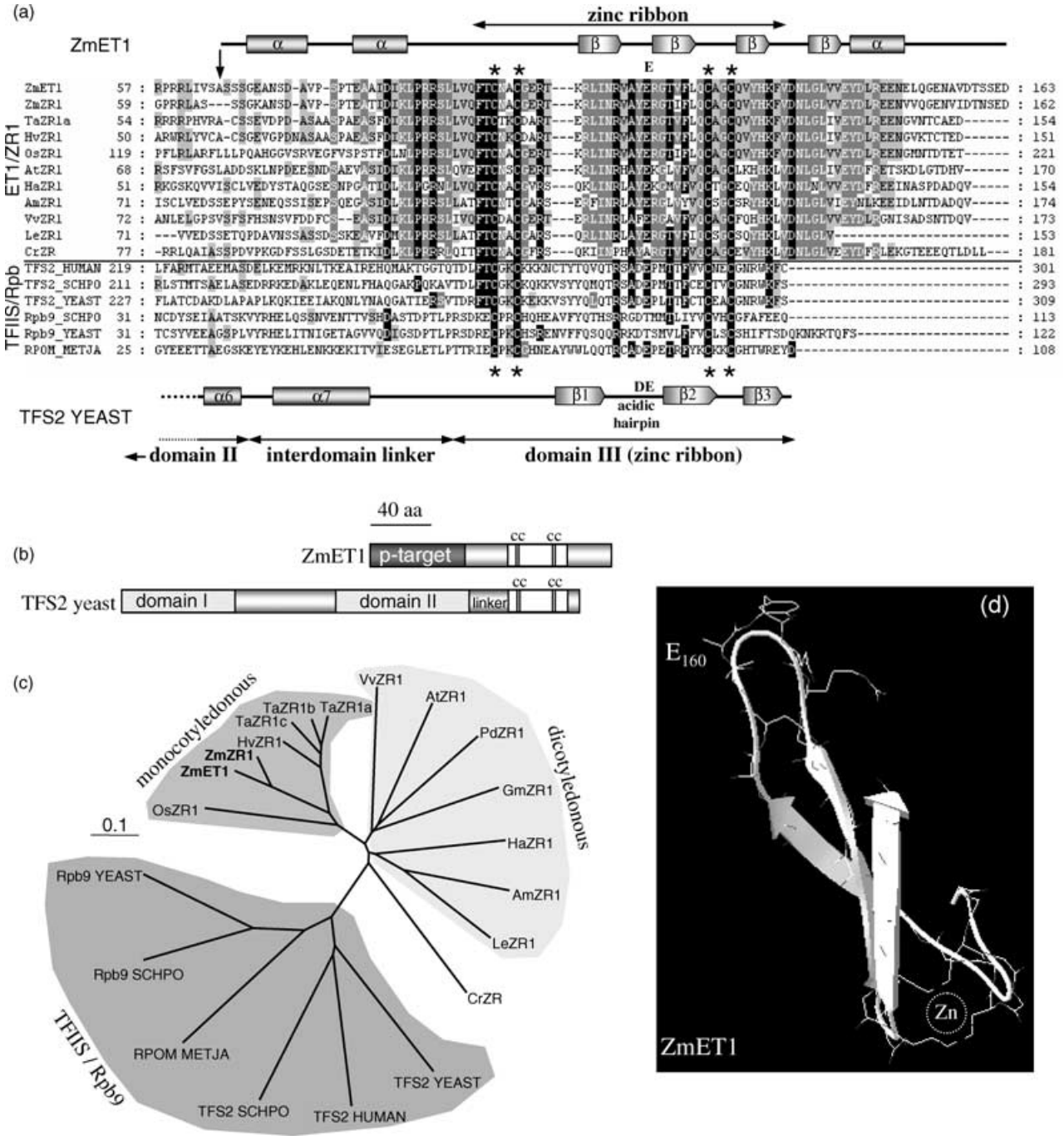

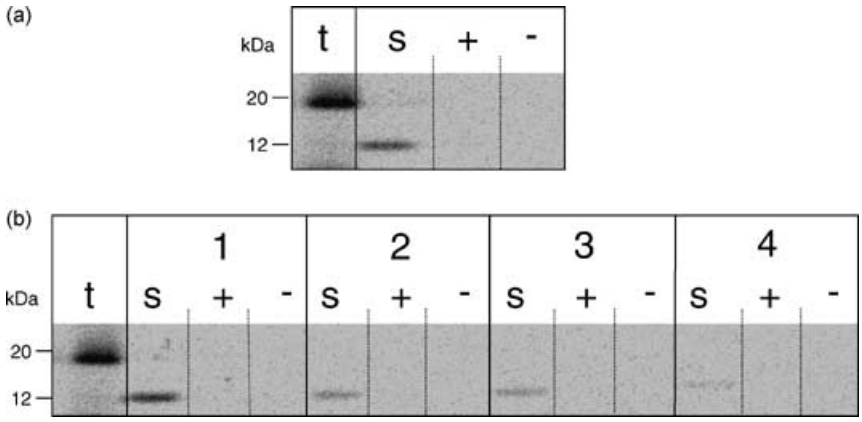

Figure 7. Chloroplast import experiments with the ET1 protein.
(a) Intact spinach chloroplasts were incubated with the *in vitro* translated and radioactively labeled ET1 protein fractionated and treated with proteases to give three different fractions. First lane (t) shows the ^{35}S-labeled *in vitro* translated ET1 protein (approximately 20 kDa), followed by the stroma (S) and thylakoid membrane fractions (+) and (−) of the chloroplast import experiment. The (+) fraction represents the membrane fraction treated with protease (thermolysin). The (−) fraction represents the membrane fraction not treated with the protease.
(b) ET1 chloroplast import experiment with a competitor protein. An unlabelled 33 kDa subunit of the oxygen evolving complex was added in increasing concentrations (from 1 to 4) to the ET1 chloroplast import experiment as described in (a). Concentrations of competitor protein (in 7 M urea) present in samples 1–4 are 0, 1, 2, and 4 μM, respectively. For abbreviations, see (a).

fraction (Figure 7b), clearly showing that the ET1 protein is imported into the stroma of chloroplasts via the general import pathway.

The ET1 protein is a component of the TAC of chloroplasts

Computational analysis of ET1 and its similarity to TFIIS suggested a putative function of the protein in the transcriptional apparatus of plastids. Upon lysis of plastids, transcriptional activity is found in the soluble fraction and in the membrane fraction (Igloi and Kössel, 1992). The latter fraction is tightly bound to the plastid DNA and is capable of elongating transcripts that have already been initiated *in vivo* (Hallick *et al.*, 1976). Compared to the original crude TAC fraction (Hallick *et al.*, 1976) the specific activity of this TAC may be significantly enhanced by different purification steps (Krause and Krupinska, 2000). A crude fraction (TACI) and a highly purified fraction (TACII) were prepared from chloroplasts of the wild type (*Et1*) and of non-virescent *et1* mutant (*et1-R*) leaves collected from about 4-week-old plants, respectively. Transcriptional activity was determined by incorporation of ^{32}P-labeled nucleotides into transcripts initiated before preparation of TAC (Krupinska and Falk, 1994). Maize TACII fractions had a fourfold higher specific activity than TACI fractions. The relative activity of both *et1-R*-derived TAC fractions was less than half when compared to the relative activity of the corresponding TAC fractions from wild-type leaves (Figure 8a). These differences in the overall transcriptional activity are not reflected by qualitative changes in the composition of transcripts. The latter has been shown by hybridization of TAC-derived transcripts with 22 selected plastid genes represented on a DNA-dot-blot filter (provided as Supplementary Material). The filter carried probes of genes with either plastid-encoded RNA

Figure 6. Similarity, predicted structure, and phylogenetic relationship of ET1.
(a) The mature ET1 protein (ZmET1) and putative ZR domains of members of the ZR1-protein family were aligned manually with the ZR domains of TFIIS and Rpb9 proteins. The putative cleavage site of the ET1 plastid transit sequence is marked with an arrow. Identical or physicochemically similar amino acids among the proteins are shaded. The four ZR-specific cysteines are indicated with (∗). The α-helices and β-strands in the C-terminal region of the yeast TFIIS protein are shown below the alignment according to Kettenberger *et al.* (2003). The two conserved acidic residues (**D,E**) in the acidic hairpin are given. The predicted secondary structure of the mature ET1 is shown above the alignment. The conserved glutamate (**E**) is marked. For sequence legends, see (c).
(b) Schematic comparison between the domain structure of the maize protein ZmET1 and the yeast protein TFIIS. P-target, plastid targeting signal.
(c) Phylogenetic analysis of the ZR1 family and TFIIS-related proteins. Similarity and phylogenetic relationship of proteins was calculated using CLUSTALX and was visualized using TREEVIEW. RPOM_METJA was used as outgroup. Non-annotated ZR1 sequences that had been identified in the expressed sequenced tag (EST) databases or in the *Arabidopsis* genome are named with a two-letter prefix added. At, *A. thaliana*; Am, *Antirrhinum majus*; Cr, *C. richardii*; Gm, *Glycine max*; Ha, *Helianthus annuus*; Hv, *Hordeum vulgare*; Le, *Lycopersicon esculentum*; Os, *Oryza sativa*; Pd, *Prunus dulcis*; Ta, *Triticum aestivum*; Vv, *Vitis vinifera*; and Zm, *Z. mays*; TFS2_HUMAN, *Homo sapiens*, Transcription elongation factor S-II (spP23193); TFS2_SCHPO, *Schizosaccharomyces pombe* (spP49373); TFS2_YEAST, *Saccharomyces cerevisiae* (spP07203); Rpb9_SCHPO, *S. pombe* RNA polymerase II subunit 9 (spO74635); Rpb9_YEAST, *S. cerevisiae* (spP27999); and RPOM_METJA, *Methanococcus jannaschii*, DNA-directed RNA polymerase subunit M (spQ58548).
(d) Tertiary structure prediction of the ZR domain of ET1, using the yeast TFIIS domain III (ZR, see a,b) as template for modeling. The position of the conserved glutamate (E_{116}) is indicated and the region of the zinc ion is marked manually.

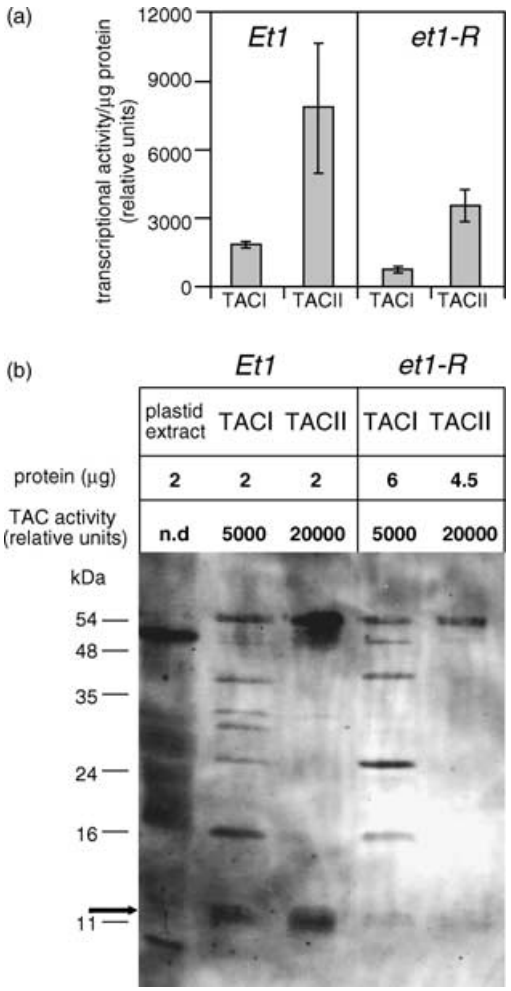

Figure 8. Relative transcriptional activities of TAC fractions from *Et1* and *et1-R* plastids and immunodetection of ET1

(a) Crude (TACI) and highly enriched (TACII) transcriptionally active chromosome preparations from isolated chloroplasts of *Et1* and *et1-R* plants were assayed for relative transcriptional activity. Values with SDs are means of two independent experiments.

(b) Proteins from wild-type chloroplasts and TAC fractions (see a) were size fractionated using PAGE and subjected to a Western blot with a polyclonal antibody raised against an ET1-derived peptide. Equal amounts of relative transcriptional activity were loaded for the TACI (5000 U) and TACII (20 000 U) fractions of *Et1* and *et1-R*. This corresponds to a two- to threefold higher amount of protein for *et1-R*. A strong band of the expected molecular size of the processed ET1 protein of approximately 12 kDa is visible in TAC-enriched fractions from *Et1* wild-type seedlings (arrow). The intensity of the signal correlated with the transcriptional activity. In TAC fractions of *et1-R* seedlings, only a very faint band, most likely because of a cross-reaction of the antibody with an ET1 homolog, could be detected.

polymerase (PEP; *psa*A, *psb*A, *psb*C–*psb*F, *rbc*L, and *ndh*H) or nuclear-encoded phage-type RNA polymerase (NEP) promoter (*rpo*A, and *rpo*B/C operon) and of genes possessing both types of promoters (*rrn* operon, *atp*B). Relative transcriptional activities among the selected genes in both cases were similar to those observed in mature chloroplasts derived from fully expanded primary foliage leaves of barley (Krupinska and Falk, 1994). Taken together, these data suggest that the lack of ET1 protein leads to a reduced transcription rate without affecting the gene specificity of the transcriptional apparatus.

To investigate whether the ET1 protein belongs to the TAC fraction, TAC proteins derived from wild-type and *et1-R* mutant chloroplasts were analyzed immunologically with a polyclonal antibody raised against a deduced ET1 peptide sequence. The specificity of the antibody was shown before by precipitation of the *in vitro* translated ET1 pre-protein (data not shown). Western analyses were performed with total plastid proteins and with proteins derived from crude (TACI) and highly purified (TACII) TAC fractions, respectively (Figure 8b). As shown before for the purified TAC fraction prepared from spinach (Krause and Krupinska, 2000) in the TACII fraction derived from maize wild-type and mutant chloroplasts, 30–40 polypeptides were detectable by silver staining. TACI and TACII samples loaded onto the gel had similar protein contents but different transcriptional activities, respectively. While the amounts of TACI corresponded to 5000 U relative transcriptional activity, the amounts of TACII corresponded to 20 000 U of relative transcriptional activity (Figure 8a,b). Immunological analyses clearly revealed the presence of a protein of 12 kDa in TAC fractions derived from wild-type chloroplasts. The expected molecular weight of the processed ET1 protein is 12 kDa. The protein is highly enriched with the TAC fractions as it is not detectable in unfractionated protein extracts from chloroplasts (Figure 8b; arrow). Because of its higher relative abundance in TACII compared to TACI, the abundance of the 12 kDa protein in wild-type chloroplasts rather correlates with the relative transcriptional activity than with the amount of loaded protein, which is equal for TACI and TACII (Figure 8b). In comparison to the TAC fractions from wild-type chloroplasts, TAC fractions from the *et1-R* mutant plastids gave only very faint signals after immunodetection, although higher protein amounts had been loaded on the gel because of the reduced transcriptional activity of *et1-R* TAC fractions (Figure 8a,b). As the peptide antibody is directed against a region present in both, ET1 and its homolog ZmZR1, it is conceivable that the weak detected signal is caused by a cross-reaction of the antibody with the ZmZR1 protein.

These results suggest that ET1 is a constituent of the TAC and that its abundance correlates with the rate of overall transcriptional activity in this fraction.

Discussion

Isolation of the et1 *gene*

The cloning of genes via transposon tagging is a well-established procedure in maize (review: Chomet, 1994;

Wienand *et al.*, 1982). To clone the affected gene of a *Mu*-induced mutant, a genomic fragment containing a transposon-specific sequence co-segregating with the mutant phenotype had to be identified. Several independent *Mu*-induced *et1* alleles were used for the isolation and investigation of the *et1* locus. The *et1* gene was characterized through the molecular analysis of six different *et1* mutants. The presence of a *Mu8* element in the 5′ UTR of four alleles, viz *et1-M3*, *et1-M10*, *et1-M12*, and *et1-M15*, and a *Mu1* element within the ORF in exon1 of the *et1-M16* allele was identified (Figure 4a). No *Mu* inserts were detected in wild-type *Et1* genes.

Germinal revertants or somatic revertant sectors can provide further evidence of the successful cloning of a gene. As germinal revertants are rarely observed for *Mu*-induced mutants, somatic revertant sectors were often used to show that the excision of the element from the respective locus restores the gene activity and is responsible for wild-type phenotype in these sectors. This was shown for *et1-M3* by analyzing a revertant leaf sector. The *Mu8* element was found to be missing from the *et1* locus in the green revertant sectors of *et1-M3* leaves; however, duplicated target sites of insertion (footprints) were still present (Figure 4b). As the element had integrated into the 5′ UTR of the gene, its excision did not interfere with the transcription and translation of the gene.

The *et1* phenotype is observed in kernels and also during the first 2 weeks after seedling germination. Expression of the *Et1* gene was detected during endosperm development in wild-type plants at 10, 15 and 20 DAP. Generally, this period comprises the stages of endosperm differentiation and kernel desiccation, which begin after complete cellularization, taking place at 4 DAP (Becraft and Asuncion-Crabb, 2000; Kranz *et al.*, 1998). Starch synthesis also takes place about 2 weeks or less after fertilization (Kiesselbach, 1949). In contrast to the wild type, in all the analyzed mutants, no *Et1* expression was observed during this developmental period. Thus, the absence of *Et1* transcripts in the mutants very likely leads to the aberrant development of the endosperm during this stage of development. In combination, the presented data demonstrate the successful cloning of the *Et1* gene.

The *et1-R* mutant allele was derived from an X-ray-treated population. Molecular analysis of genomic clones in *et1-R* indicated that rearrangements and deletions of the locus apparently occurred during the mutation event in this line (Figure 3). The irradiation apparently deleted the entire coding region of the *et1* gene, leaving only the promoter region intact. Hence, *et1-R* is expected to be a null allele. This is surprising given that the *et1-R* allele conditions a 'weaker' mutant phenotype than the *et1-M* alleles. One possible explanation takes into account the fact that the *et1* mutants originated from different genetic backgrounds. Differential activities because of allelic variations of an *et1* homolog might be responsible for the phenotypic variations in these lines. A high degree of allelic divergence and a differential gene expression because of line-dependent allelic variation is a characteristic feature of maize (Fu and Dooner, 2002; Kim and Krishnan, 2003; Song and Messing, 2002). It could also be that in phenotypically severe *et1* mutant lines, *Zmzr1* expression is repressed, whereas in only some (e.g. *et1-R*) weak expression is going on. Such an observation has been made in the analysis of the anthocyanin biosynthesis repressor gene *intensifier1* (Burr *et al.*, 1996).

Microscopic examinations of the developing endosperm of *et1-R* mutant kernels (Figure 1) revealed that the effect of the *et1* mutation appears to be restricted mainly to small dispersed radial sectors of endosperm radiating out from the center up to the periphery (Figure 1e,f,h). The leaves of the *et1* mutant show a temporary phenotype that depends on the developmental stage of the plant. Therefore, it is also conceivable that another gene or a set of genes might take over the role of *Et1* and restore normal plastid development during later stages of leaf development. A specific spatial or temporal expression of these genes could also be responsible for the observed phenotype in kernels. Indeed, such a close *Et1* homolog was identified in the *et1-R* line (*Zmzr1*; Figure 6). The transcribed regions of *Et1* and *Zmzr1* are very similar, whereas the promoter sequences of both genes are highly variable pointing to a different control of gene expression for both genes (data not shown). Expression of the *Et1* gene in seedlings was repressed in the dark (Figure 5b), which is in accordance with a function of the gene product during chloroplast development. Although the *Zmzr1* cDNA was cloned from a cDNA library of *et1-R* kernels, several attempts to analyze the *Zmzr1* expression by Northern analysis failed so far, most likely because of a very low abundance of the corresponding mRNA. Accordingly, it was only possible to amplify *Zmzr1* corresponding cDNA fragments by two successive rounds of RT-PCR from the *et1-R* cDNA library (data not shown). As expression of the *Zmzr1* gene is not detectable in total RNA of either light- or dark-grown *et1-R* seedlings, the level of the ET1 homolog in the *et1* mutants may be not sufficient to fully compensate for the function of ET1 during chloroplast development. In agreement with these findings, only a faint 12-kDa protein was detected in TAC fractions derived from *et1-R* plastids by the antibody, which is specific for a peptide sequence included in both ET1 and ZmZR1.

Analogously to *et1*, it has been shown that mutations in the gene of the maize chloroplast membrane protein high chlorophyll fluorescence 106 (*HCF106*) caused by the insertion of *Mu* elements could partially be compensated by the closely related homolog *HCF106c*. This homolog has been mapped to a region that is part of the most recent set of segmental duplications in the maize genome (Settles *et al.*, 2001). It is conceivable that *Et1* and *Zmzr1* might be

connected in a similar evolutionary way. This is further supported by a comparison between the identified putative ZR1 proteins, which suggest that in most plants only one *Zr1* gene is present, e.g. AtZR1 in *Arabidopsis*, whereas more than one putative ZR1 protein could only be found in maize (ET1 and ZmZR1) and in the polyploid plant wheat (TaZR1a–TaZR1c; Figure 6c).

Role of the ET1 protein in the plastids

The pleiotropic effect of the *et1* mutation, affecting both amyloplast and chloroplast development, led to the hypothesis that the gene might be involved in an essential process common to development of amyloplasts as well as chloroplasts. Chloroplast import experiments demonstrated that the ET1 protein is indeed targeted to the stroma of plastids. Therefore, ET1 is the first described ZR-containing protein in this organelle.

Comparison of the ET1 protein to online databases and its *in silico* structural analysis revealed that it exhibits some similarity to C-terminal ZR domains of proteins interacting with nucleic acids, e.g. that of the eukaryotic RNA Pol II subunit Rpb9 (Figure 6a) and the transcription factor TFIIB (Chen *et al.*, 2000; Hemming *et al.*, 2000; data not shown). Highest similarity was found to the ZR domain of the eukaryotic transcription elongation factor TFIIS (Figure 6a). This factor is composed of an N-terminal domain I, a central domain II, and the C-terminal ZR (domain III) that contains a protruding acidic β-hairpin turn (Figure 6b). The ZR domain is an ubiquitious motif in the archaeal as well as in the eukaryotic transcription machinery (Chen *et al.*, 2000). Furthermore, Männistö *et al.* (2003) showed that a ZR containing transcriptional regulator is encoded by the bacteriophage PM2 genome and is capable of regulating the eubacterial RNA polymerase. TFIIS in eukaryotes and its functional counterpart GreB in bacteria are the only known transcription factors that are capable of restarting arrested RNA polymerases, thereby ensuring efficient mRNA synthesis (Conaway *et al.*, 2003; Uptain *et al.*, 1997; Wind and Reines, 2000). RNA elongation is blocked when the RNA transcript loses contact with the DNA template (Erie, 2002; Shilatifard *et al.*, 2003). TFIIS mediates the restart of the RNA Pol II by a conformational change in the active center of Pol II, leading to the activation of its intrinsic RNA nuclease activity. During the conformational change, the acidic residues of the ZR β-hairpin are positioned into the active site (Kettenberger *et al.*, 2003). Because of the TFIIS promoted cleavage of a displaced 3′ end of the mRNA, a new 3′ end that is properly base paired with the DNA is produced and can be elongated by the polymerase (Uptain *et al.*, 1997; Wind and Reines, 2000).

Plastid transcriptional activity can be detected in two fractions, a soluble and a membrane fraction (Igloi and Kössel, 1992). In the latter fraction, which is called TAC, the transcriptional apparatus is tightly associated with the plastid DNA and is capable of elongating transcripts that have been already initiated *in vivo* (Hallick *et al.*, 1976). Western analysis demonstrated that the ET1 protein belongs to the TAC fraction and that the abundance of ET1 correlates with the relative transcriptional activity of the complex (Figure 8b). In the *et1-R* mutant line, the relative transcriptional activity of both a crude and a highly purified TAC fraction is significantly reduced compared to wild-type plants (Figure 8a). As the TAC fractions were prepared from non-virescent green leaves of the mutant, the differences in plastid transcriptional activity are not likely to be caused by secondary effects of the *et1* mutation.

Despite the differences in the rate of overall transcription, the relative transcriptional activities of different plastid genes in this fraction are similar as investigated by hybridization of *in vitro* elongated TAC transcripts with selected genes (data not shown). These results indicate that the ET1 protein stimulates overall transcriptional activity and does not affect the relative transcription of specific genes. Based on the structural model that has been published for the interaction of TFIIS with RNA Pol II in yeast (Kettenberger *et al.*, 2003) and GreB with the eubacterial RNA polymerase (Opalka *et al.*, 2003), a similar mechanism of interaction with a plastid RNA polymerase might be considered for the ZR domain of ET1. Although the ZR domain of ET1 shows the highest similarity to that of TFIIS when compared to other ZR containing transcriptional regulators from the database, it could not be excluded that ET1 function in plastids might differ from that of TFIIS.

Plastids possess at least two different types of RNA polymerases (Bligny *et al.*, 2000; Hedtke *et al.*, 2000; Maliga, 1998; review: Hess and Börner, 1999). If ET1 is influencing plastid transcription, it could do so by acting as a regulatory subunit of at least one of these RNA polymerases. So far, it has been shown that the TAC fraction contains the PEP of the eubacterial type (Suck *et al.*, 1996). Transcription of housekeeping genes by the TAC-associated polymerase(s) (Igloi and Kössel, 1992; Krupinska and Falk, 1994) however suggests that the NEP is included in the fraction, too. ZR-like proteins have been found to be part of eukaryotic as well as of archaeal and prokaryotic transcriptional complexes (Chen *et al.*, 2000). Even a bacteriophage encodes a ZR-containing factor that has been shown to regulate transcription by the eubacterial RNA polymerase (Männistö *et al.*, 2003).

Based on the sequence comparison of ET1 with other proteins that contain ZR domains and its high sequence similarity to the different identified plant proteins, it appears that ET1 is the first described member of a family of small ZR-containing plastid proteins.

The phenotype observed in leaves of *et1-R* mutants and the light-dependent expression of the *Et1* gene is in accordance with the hypothesis that ET1 functions similar to

TFIIS and GreB as a regulator of transcription elongation. It is interesting that besides chloroplast development in the leaves also endosperm development is impaired in the *et1-R* mutants. This suggests that plastid gene expression is required for development of functional amyloplasts.

As already shown by Baumgartner *et al*. (1989) with barley primary foliage leaves, proper chloroplast development in the light is associated with a tremendous increase in the level of plastid gene expression. This is achieved by an increase of both the copy number of plastid DNA and the rate of transcription. Timing and level of plastid gene expression is also impaired in the *abc1* mutant of *Arabidopsis thaliana*, which has a pale-green leaf phenotype resembling the phenotype of the *et1-R* mutant (Shirano *et al*., 2000). In case of the *abc1* mutant, the phenotype is caused by a mutation in the gene encoding sigma factor SigB. While nuclear-encoded SigB is of prokaryotic origin as its cognate RNA polymerase (PEP), ET1 with its ZR domain is of eukaryotic origin. According to Sato's model of discontinuous evolution of plastid nucleoids (Sato, 2001), the plastid genetic machinery has lost many prokaryotic proteins and has acquired nuclear-encoded eukaryotic-type proteins, e.g. the PEND protein, which is belonging to the bZIP proteins (Sato, 2001; Sato *et al*., 1998). Another example for a protein of eukaryotic origin with a function in plastid nucleoids is the coiled-coil DNA-binding protein MFP1, which seems to function as a nucleoid anchor at the interface to the thylakoid membranes (Jeong *et al*., 2003).

Current experiments aim at identifying proteins interacting with the ET1 protein. Moreover overall RNA levels will be compared between the wild type and *et1* mutant at different stages of plastid development. In addition, analyses of a *zr1* knockout mutant of *A. thaliana* are in progress.

Experimental procedures

Basic molecular biology techniques, unless otherwise specified, were conducted according to Sambrook *et al*. (1989).

Maize stocks

Wild-type *Et1* maize inbred lines used in these studies were LC (a color-converted W22 line; Wienand *et al*., 1986), B73, and H99. The *Mu*-induced alleles *et1-M1*–*et1-M10* have been described previously by Scanlon *et al*. (1994). The allele *et1-M12* was kindly provided by Phil Stinard (Maize Genetics Cooperation Stock Center, Urbana, IL, USA). The mutants *et1-M15* and *et1-M16* were isolated as described below. Unless otherwise noted, maize plants were grown in a greenhouse in Hamburg with 16 h of light at 25°C under a relative humidity of 55–95%.

Directed tagging of Et1

The mutants *et1-M15* and *et1-M16* were isolated from the cross *A1 Et1/A1 Et1 Mu* × *a1 et1-R/a1 et1-R*. The female parent (listed first) was an active *Mu* stock that had been maintained as described by Stinard *et al*. (1993). Both parents of this cross were planted in an isolation plot. The female parent was manually emasculated prior to anthesis. Colored, etched kernels identified in the progeny of this cross were test-crossed to *et1-R* to establish that they indeed carried novel *et1-M* alleles.

Southern and Northern analyses

Maize genomic DNA was isolated following the protocol provided by Dellaporta *et al*. (1983). Total RNA was isolated from different plant parts as described previously by Weisshaar *et al*. (1991). Southern and Northern blot hybridizations were carried out under stringent conditions according to Sambrook *et al*. (1989). Either the complete *Et1* cDNA or the 3′ UTR of the gene were used as a probe for Northern blots.

AIMS analysis

A modified version (Lauert *et al*., 1999) of the AIMS analysis (Frey *et al*., 1998) was used to analyze *et1-M3* mutants (*et1-R*/*et1-M3*) along with their wild-type siblings (*et1-R*/*Et1*). The experiment was performed using three different four-base restriction cutters individually, i.e. *Hpa*II, *Mse*I, and *Hin*PI.

Construction and screening of genomic and cDNA libraries

Genomic libraries were constructed with lambda Fix II vector (Stratagene, Heidelberg, Germany) following manufacturer's protocols. DNA was isolated from individuals of the following genotypes for this purpose: LC, *et1-M3*/*Et1*, *et1-R*, *et1-M16*/*et1-R*, and *et1-M15*/*et1-R*. A cDNA library was constructed with the mRNA isolated from LC kernels harvested at 13, 17, 19, 20, 22, 25, and 28 DAP. Equal amounts of total RNA from these probes were mixed prior to the isolation of poly(A)+ mRNA using oligo-dT cellulose. A lambda ZAPII (Stratagene) vector was used and the library was constructed using an oligo-dT primer for the first-strand synthesis as instructed by the manufacturer. All libraries were screened following standard protocols (Sambrook *et al*., 1989). A 171-bp *Hpa*II/G fragment, identified in the AIMS analysis to co-segregate with the *et1-M3* mutation, was used as a probe to screen the *et1-M3*/*Et1* genomic library. A 2.5-kbp *Hin*dIII–*Xho*I genomic fragment (Frag 3 in Figure 3) was then used to screen an *et1-R*/*et1-M16* as well as an LC genomic library. The *et1-M15* library was screened with the full-size cDNA clone c*Et1*-9.

Restriction fragment length polymorphism mapping in recombinant inbreds

The 2.5-kbp *Hin*dIII–*Xho*I fragment (Figure 3) was used as a hybridization probe to map the *et1* gene in two recombinant inbred populations Cm37XT232 (48 individuals) and Tx303 × Co159 (41 individuals) (Burr and Burr, 1991; Burr *et al*., 1988). This probe identified a *Bam*HI polymorphism in these populations.

Cloning of et1-M3 Revertant-1 *integration site and PCR analysis*

A revertant sector (dark-green on a pale-green background) of a leaf of an *et1-M3*/*et1-R* plant was dissected and genomic DNA was

isolated using the DNeasy Plant Mini Kit (Qiagen, Hilden, Germany) and according to the manufacturer's instructions. The following PCR was performed with the isolated genomic DNA: DNA (100 ng); 10 pmol each of primers *Et*-PCR1 and *Et*-PCR2; 0.625 mM dNTPs; and 2.5 U Taq polymerase (Life Technologies, Karlsruhe, Germany) in a total volume of 50 μl. The PCR program was as follows: 94°C for 5 min, 85°C/hold (addition of the primers); 29× (94°C for 45 sec; 65°C for 45 sec, and 72°C for 1 min); 1× (94°C for 45 sec, 65°C for 45 sec, and 72°C for 10 min); and 4°C/hold. After completion of the PCR, the products were purified with the QIAquick PCR Purification Kit (Qiagen) as instructed by the manufacturer. The products were then blunt ended with Klenow polymerase, extracted with phenol and chloroform, and run over a Sephadex G-25 column. The resulting purified blunt-ended products were ligated into *Eco*RV-cut pZero (Invitrogen, Karlsruhe, Germany). Clones carrying the appropriate insert were found in a colony hybridization experiment using c*Et1*-9 as probe. Positive clones were sequenced.

Primers used were: *Et*-PCR1, 5′-GAAGCGGAGACAATGAGCCTCCTTG-3′; and *Et*-PCR2, 5′-TCCTTGGGCTAACGGTGGACAG-3′. The 5′ end of *Et*-PCR1 is 78 bases upstream of the first nucleotide and *Et*-PCR2 expands from position 207 to 183 of the cDNA c*Et1*-9, respectively.

Nucleic acid sequencing

Plasmid subclones were sequenced based on the didesoxynucleotide chain termination method using the Big Dye Terminator sequencing kit (Perkin Elmer/Applied Biosystems, Weiterstadt, Germany) and specific primers based on the manufacturer's protocols, and analyzed on an automated DNA sequencer (model 377; Applied Biosystems).

Sequence analyses and database searches

Sequence alignments were performed by hand using GENEDOC 2.6.001 (Nicholas and Nicholas, 1997). Phylogenetic relationships were calculated using CLUSTALX 1.8.1 (Thompson *et al.*, 1997) and depicted using TREEVIEW 1.6.6 (Page, 1996). Database searches were conducted online with the actual releases of the available protein and nucleic acid databases with the BLAST algorithm (Altschul *et al.*, 1990, 1997). Computational analyses for the prediction of intracellular protein localization signals were conducted using the programs TARGETP, CHLOROP, and PSORT (Emanuelsson *et al.*, 1999, 2000; Nakai and Kanehisa, 1992).

The similarity of ET1 to the ZR domain of TFIIS was identified through the Pfam database of hidden Markov Models (Bateman *et al.*, 1999) available at the PROSITE database. The predicted secondary structure of ET1 was derived from the consensus of calculations using 14 different prediction programs available online at the EXPASy Molecular Biology server (http://www.expasy.ch/tools). Tertiary structure modeling was achieved online using CPHMODELS 2.0 (Lund *et al.*, 2002) and was visualized using RASWIN 2.6 (Sayle and Milner-White, 1995).

Light and electron microscopy

The *et1* phenotype of mutant kernels was examined by preparing hand sections of the kernels and viewing under a Zeiss stereomicroscope. Twenty DAP *et1-R* kernels were examined either unstained or after violet blue staining of starch with IKI (iodide-potassium-iodide) solution. The *et1-M3/et1-R* kernels were examined by staining with methylene blue and viewing under a Zeiss stereomicroscope using UV epifluorescent light.

To examine the phenotype of young *et1-M3/et1-R* seedlings, the second youngest leaf of pale seedlings, 120 mm in height, was used. The leaf was cut into five equal (0.2–0.3 cm broad) pieces, fixed in 2.5% glutaraldehyde in 0.1 M cacodylate buffer (pH 7.0), further cut into 1–1.5 mm pieces, post-fixed in 2% OsO_4 in 0.05 M cacodylate buffer for 2 h, dehydrated in increasing concentrations of acetone (4°C), washed in 100% acetone (RT), infiltrated with Spurr's resin:acetone in 1 : 3 ratio for 1 h, followed by 1 : 1 ratio of both for 1 h, then in 3 : 1 ratio overnight, and finally with 100% Spurr's resin for 4 h (Spurr, 1969). The resin with the leaf pieces was allowed to polymerize at 70°C for 24 h. Ultrathin sections (0.05–0.1 μm) of the embedded leaves were viewed under a transmission electron microscope.

Chloroplast import experiments

The complete *Et1* cDNA c*Et1*-9 was cloned into an effective *in vitro* transcription vector pBAT possessing a rabbit β-globin leader sequence at the 5′ end of the site of cloning (Annweiler *et al.*, 1991) and transcribed with T3 polymerase based on Sambrook *et al.* (1989). The *in vitro* translation was carried out at 30°C for 90 min using the rabbit reticulocyte lysate kit (Promega, Mannheim, Germany). For this, about 5% of the synthesized mRNA was precipitated and centrifuged down, and the pellet was directly re-suspended in 12.5 μl *in vitro* translation mix (4.35 μl of H_2O; 0.9 μl of 1 M KCl; 0.25 μl of 100 mM DTT; 0.25 μl of amino acid mix (minus cysteine); 6.25 μl of reticulocyte lysate; and 0.5 μl of ^{35}S-cysteine). Afterwards, the translation mix was directly used for the chloroplast import experiment conducted using isolated spinach chloroplasts following the protocol provided by Clausmeyer *et al.* (1993). A competition experiment with the unlabeled 33-kDa protein subunit of the oxygen-evolving complex was performed according to Michl *et al.* (1994). After the import reaction, the different chloroplast protein fractions were analyzed using a resolving SDS–polyacrylamide gel prepared according to Sambrook *et al.* (1989).

Preparation of plastids and TAC

Maize was grown in the greenhouse at 22°C with 16 h light and 8 h dark. Plastids were prepared from leaves of about 4-week-old plants as described by Poulsen (1983). For extraction of proteins plastids were solubilized in 62.5 mM Tris–HCl, pH 6.8), 10% (v/v) glycerol, 1% (w/v) SDS, and 5% (v/v) β-mercaptoethanol at 95°C for 5 min. TACs of different purity were prepared as described by Krause and Krupinska (2000). TAC fractions obtained after a single gel filtration step are referred to as TACI. Highly enriched TAC fractions obtained after two subsequent gel filtration steps and ultracentrifugation are referred to as TACII. Before gel filtration, the fractions were precipitated by protamine sulfate and pellets were re-dissolved by heparin. Transcriptional activity of the TAC fractions was determined as described previously by Krupinska and Falk (1994) and Suck *et al.* (1996).

Immunological analyses

A polyclonal antibody was rised by Biogenes (Berlin, Germany) against the peptide SDAVPSPTEA-C, which was deduced from the putative ET1 protein sequence. This peptide sequence is also present in the sequence of the putative ZmZR1 protein. Plastid proteins were analyzed by SDS–polyacrylamide gel

electrophoresis (PAGE) on 16% (w/v) acrylamide gels with 'High-Tris' buffer (Fling and Gregerson, 1986). Immunological analyses after transfer of the proteins onto nitrocellulose membranes were performed as described by Humbeck *et al.* (1994).

Acknowledgements

We thank Hong Yao of the Schnable laboratory (Iowa State University) for generating the *et1* recombinant inbred mapping data and Ben Burr (Brookhaven National Laboratory, Upton, NY, USA) for analyzing these mapping data. We also thank Jürgen Berghöfer and Ralf Bernd Klösgen (Halle University) in whose laboratory the chloroplast import experiments were carried out. We acknowledge technical assistance of Wrike Peters and critical reading of the manuscript by Kirsten Krause (Institute of Botany, Kiel, Germany). This research was supported in part by a competitive grant from the United States Department of Agriculture National Research Initiative program no. 01-01869 to P.S.S. and Hatch Act and State of Iowa funds and a DFG grant (SPP1005; Wi1517/1.1–1.3).

Supplementary Material

The following material is available from http://www.blackwellpublishing.com/products/journals/suppmat/TPJ/TPJ2094/TPJ2094sm.htm

Figure S1. Transcription analysis by hybridization of TAC transcripts to DNA dot blots derived from 4-week-old leaves of wild-type (a) and *et1-R* (b) maize plants. Two identical filters carrying four concentrations (5 (1×)–320 ng (64×)) of plasmid DNA of recombinant pBluescript clones containing specfic barley or maize (∗) plastid DNA fragments and original pBluescript as control were used. Hybridization reactions were performed with the same amount of radioactively labeled TAC transcripts, and both autoradiograms were exposed for the same time. Cross-hybridization of both filters delivered identical results (data not shown).

References

Altschul, S.F., Gish, W., Miller, W., Myers, E.W. and Lipman, D.J. (1990) Basic local alignment search tool. *J. Mol. Biol.* **215**, 403–410.

Altschul, S.F., Madden, T.L., Schaffer, A.A., Zhang, J., Zhang, Z., Miller, W. and Lipman, D.J. (1997) Gapped BLAST and PSI-BLAST: a new generation of protein database search programs. *Nucl. Acids Res.* **25**, 3389–3402.

Annweiler, A., Hipskind, A. and Wirth, T. (1991) A strategy for efficient *in vitro* translation of cDNAs using the rabbit β-globin leader sequence. *Nucl. Acids Res.* **19**, 3750.

Awrey, D.E., Shimasaki, N., Koth, C. *et al.* (1998) Yeast transcript elongation factor (TFIIS), structure and function. Part II. RNA polymerase binding, transcript cleavage and read-through. *J. Biol. Chem.* **273**, 22595–22605.

Bateman, A., Birney, E., Durbin, R., Eddy, S.R., Finn, R.D. and Sonnhammer, E.L.L. (1999) Pfam 3.1: 1313 multiple alignments match the majority of proteins. *Nucl. Acids Res.* **27**, 260–262.

Baumgartner, B.J., Rapp, J.C. and Mullet, J.E. (1989) Plastid transcription activity and DNA copy number increase early in barley chloroplast development. *Plant Physiol.* **89**, 1011–1018.

Becraft, P.W. and Asuncion-Crabb, Y. (2000) Positional cues specify and maintain aleurone cell fate in maize endosperm development. *Development*, **127**, 4039–4048.

Bligny, M., Courtois, F., Thaminy, S., Chang, C.-C., Lagrange, T., Baruah-Wolff, J., Stern, D. and Lerbs-Mache, S. (2000) Regulation of plastid rDNA transcription by interaction of CDF2 with two different RNA polymerases. *EMBO J.* **19**, 1851–1860.

Burr, B. and Burr, F.A. (1991) Recombinant inbreds for molecular mapping in maize: theoretical and practical considerations. *Trends Genet.* **7**, 55–60.

Burr, B., Burr, F.A., Thompson, K.H., Albertson, M.C. and Stuber, C.W. (1988) Gene mapping with recombinant inbreds in maize. *Genetics*, **118**, 519–526.

Burr, F.A., Burr, B., Scheffler, B.E., Blewitt, M., Wienand, U. and Matz, E.C. (1996) The maize repressor-like gene *intensifier1* shares homology with the *r1/b1* multigene family of transcription factors and exhibits missspicing. *Plant Cell*, **8**, 1249–1259.

Chen, H.T., Legault, P., Glushka, J., Omichinski, J.G. and Scott, R.A. (2000) Structure of a (Cys3His) zinc ribbon, a ubiquitous motif in archaeal and eucaryal transcription. *Protein Sci.* **9**, 1743–1752.

Chomet, P.S. (1994) Transposon tagging with Mutator. In *The Maize Handbook* (Freeling, M. and Walbot, V., eds). New York: Springer Verlag, pp. 243–249.

Clausmeyer, S., Klösgen, R.B. and Herrmann, R.G. (1993) Protein import into chloroplasts. The hydrophilic lumenal proteins exhibit unexpected import and sorting specificities in spite of structurally conserved transit peptides. *J. Biol. Chem.* **268**, 13869–13876.

Coe, E.H., Jr, Neuffer, M.G. and Hoisington, W.L. (1988) The genetics of corn. In *Corn and Corn Improvement* (Sprague, G.F. and Dudley, J.W., eds). Madison: ASA, CSSA, SSSA Publishers, pp. 83–258.

Conaway, R.C., Kong, S.E. and Weliky Conaway, J. (2003) TFIIS and GreB: two like-minded transcription factors with sticky fingers. *Cell*, **114**, 272–273.

Dellaporta, S.L., Wood, J. and Hicks, J.B. (1983) A plant DNA minipreparation: version II. *Plant Mol. Biol. Rep.* **1**, 19–22.

Dietrich, C., Cui, F., Packila, M., Li, J., Ashlock, D.A., Nikolau, B.J. and Schnable, P.S. (2002) Maize *Mu* transposons are targeted to the 5′ UTR of the *gl8a* gene and sequences flanking *Mu* target site duplications exhibit non-random nucleotide composition throughout the genome. *Genetics*, **160**, 697–716.

Emanuelsson, O., Nielsen, H. and von Heijne, G. (1999) ChloroP, a neural network-based method for predicting chloroplast transit peptides and their cleavage sites. *Protein Sci.* **8**, 978–984.

Emanuelsson, O., Nielsen, H., Brunak, S. and von Heijne, G. (2000) Predicting subcellular localization of proteins based on their N-terminal amino acid sequence. *J. Mol. Biol.* **300**, 1005–1016.

Erie, D.A. (2002) The many conformational states of RNA polymerase elongation complexes and their roles in the regulation of transcription. *Biochim. Biophys. Acta*, **1577**, 287–307.

Fling, S.P. and Gregerson, D.S. (1986) Peptide and protein molecular weight determination by electrophoresis using a high-molecular tris buffer system without urea. *Anal. Biochem.* **155**, 83–88.

Frey, M., Stettner, C. and Gierl, A. (1998) A general method for gene isolation in tagging approaches: amplification of insertion mutagenised sites (AIMS). *Plant J.* **13**, 717–721.

Fu, H. and Dooner, H.K. (2002) Intraspecific violation of genetic colinearity and its implications in maize. *Proc. Natl. Acad. Sci. USA*, **99** (14), 9573–9578.

Hallick, R.B., Lipper, C., Richards, O.C. and Rutter, W.J. (1976) Isolation of a transcriptionally active chromosome from chloroplasts of *Euglena gracilis*. *Biochemistry*, **15**, 3039–3045.

Hedtke, B., Börner, T. and Weihe, A. (2000) One RNA polymerase serving two genomes. *EMBO Rep.* **1**, 435–440.

Hemming, S.A. and Edwards, A.M. (2000) Yeast RNA polymerase II subunit RPB9: mapping of domains required for transcription elongation. *J. Biol. Chem.* **275**, 2288–2294.

Hemming, S.A., Jansma, D.B., Macgregor, P.F., Goryachev, A., Friesen, J.D. and Edwards, A.M. (2000) RNA polymerase II subunit Rpb9 regulates transcription elongation *in vivo*. *J. Biol. Chem.* **275**, 35506–35511.

Hess, W.R. and Börner, T. (1999) Organellar RNA polymerases of higher plants. *Int. Rev. Cytol.* **190**, 1–59.

Humbeck, K., Melis, A. and Krupinska, K. (1994) Effects of chilling in chloroplast development in barley primary foliage leaves. *J. Plant Physiol.* **143**, 744–749.

Igloi, G.L. and Kössel, H. (1992) The transcriptional apparatus of chloroplasts. *Crit. Rev. Plant Sci.* **10**, 525–558.

Jeong, S.Y., Rose, A. and Meier, I. (2003) MFP1 is a thylakoid-associated, nucleoid-binding protein with a coiled-coil structure. *Nucl. Acids Res.* **17**, 5175–5185.

Kettenberger, H., Armache, K.-J. and Cramer, P. (2003) Architecture of the RNA polymerase II-TFIIS complex and implications for mRNA cleavage. *Cell*, **114**, 347–357.

Kiesselbach, T.A. (1949) *The Structure and Reproduction of Corn*. Lincoln and London: University of Nebraska Press.

Kim, W.S. and Krishnan, H.B. (2003) Allelic variation and differential expression of methionine-rich δ-zeins in maize inbred lines B73 and W23a1. *Planta*, **217**, 66–74.

Kranz, E., von Wiegen, P., Quader, H. and Lörz, H. (1998) Endosperm development after fusion of isolated, single maize sperm and central cells *in vitro*. *Plant Cell*, **10**, 511–524.

Krause, K. and Krupinska, K. (2000) Molecular and functional properties of highly purified transcriptionally active chromosomes from spinach chloroplasts. *Physiol. Plant.* **109**, 188–195.

Krupinska, K. and Falk, J. (1994) Changes in RNA-polymerase activity during development and senescence of barley chloroplasts. Comparative analysis of transcripts synthesized either in run-on assays or by transcriptionally active chromosomes (TAC). *J. Plant Physiol.* **143**, 298–305.

Lauert, P., da Costa e Silva, O. and Wienand, U. (1999) The use of Thermomixer Comfort for AIMS. *Eppendorf Appl.* **N. 15**, 1–4.

Lund, O., Nielsen, M., Lundegaard, C. and Worning, P. (2002) CPHmodels 2.0: X3M a computer program to extract 3D models. Abstract in the CASP5 conference: A 102.

Maliga, P. (1998) Two plastid RNA polymerases of higher plants: an evolutionary story. *Trends Plant Sci.* **3**, 4–6.

Männistö, R.H., Grahn, A.M., Bamford, D.H. and Bamford, J.K.H. (2003) Transcription of bacteriophage PM2 involves phage-encoded regulators of heterologous origin. *J. Bacteriol.* **185** (11), 3278–3287.

Michl, D., Robinson, C., Shackleton, J.B., Herrmann, R.G. and Klösgen, R.B. (1994) Targeting of proteins to the thylakoids by bipartite presequences: CFoII is imported by a novel, third pathway. *EMBO J.* **13**, 1310–1317.

Nakai, K. and Kanehisa, M. (1992) A knowledge base for predicting protein localization sites in eukaryotic cells. *Genomics*, **14**, 897–911.

Neuffer, M.G., Coe, E.H. and Wessler, S.R. (1997) *Mutants of Maize*. New York: Cold Spring Harbour Laboratory Press.

Nicholas, K.B. and Nicholas, H.B., Jr (1997) GeneDoc: a tool for editing and annotating multiple sequence alignments. http://www.psc.edu/biomed/genedoc/.

Opalka, N., Chlenov, M., Chacon, P., Rice, W.J., Wriggers, W. and Darst, S.A. (2003) Structure and function of the transcription elongation factor GreB bound to bacterial RNA polymerase. *Cell*, **114**, 335–345.

Page, R.D.M. (1996) An application to display phylogenetic trees on personal computers. *CABIOS*, **12**, 357–358.

Poulsen, C. (1983) The barley chloroplast genome: physical structure and transcriptional activity *in vivo*. *Carlsberg Res. Commun.* **48**, 57–80.

Ramesh, S.V., Santa Kumari, A.S. and Reddy, A.R. (1984) Photoacoustic and physiological studies on a maize mutant: a delay in leaf pigment synthesis in virescent seedlings. *Biochem. Int.* **9**, 121–128.

Sambrook, J., Fritsch, E.F. and Maniatis, T. (1989) *Molecular Cloning: a Laboratory Manual*. New York: Cold Spring Harbor Laboratory Press.

Sangeetha, H.G. and Reddy, A.R. (1991) Genetic and biochemical analysis of the *Etched* (*et*) mutant of *Zea mays* L. *Maydica*, **36**, 343–354.

Sangeetha, H.G., Ramesh, S.V., Jayaram, C. and Reddy, A.R. (1986) Studies on chlorophyll and protein accumulation in thylakoids and chloroplast development in virescent seedlings of a maize mutant. *Biochem. Int.* **12**, 181–188.

Sato, N. (2001) Was the evolution of plastid genetic machinery discontinuous? *Trends Plant Sci.* **6** (4), 151–155.

Sato, N., Oshima, K., Watanabe, A., Ohta, N., Nishiyama, Y., Joyard, J. and Douce, R. (1998) Molecular characterization of the PEND protein, a novel bZIP protein present in the envelope membrane that is the site of nucleoid replication in developing plastids. *Plant Cell*, **10**, 859–872.

Sayle, R. and Milner-White, E.J. (1995) RasMol: biomolecular graphics for all. *Trends Biochem. Sci.* **20** (9), 374.

Scanlon, M.J., James, M.G., Stinard, P.S., Myers, A.M. and Robertson, D.S. (1994) Characterization of ten new mutations of the maize *Etched-1* locus. *Maydica*, **39**, 301–308.

Settles, A.M., Baron, A., Barkan, A. and Martienssen, R.A. (2001) Duplication and suppression of chloroplast protein translocation in maize. *Genetics*, **157**, 349–360.

Shilatifard, A., Conaway, R. and Conaway, J.W. (2003) Structural basis for the species-specific activity of TFIIS. *J. Biol. Chem.* **275**, 36541–36549.

Shirano, Y., Shimada, H., Kanamura, K. *et al.* (2000) Chloroplast development in *Arabidopsis thaliana* requires the nuclear-encoded transcription factor Sigma B. *FEBS Lett.* **485**, 178–182.

Soll, J. and Tien, R. (1998) Protein translocation into and across the chloroplastic envelop membranes. *Plant Mol. Biol.* **38**, 191–207.

Song, R. and Messing, J. (2002) Gene expression of a gene family in maize based on noncollinear haplotypes. *Proc. Natl. Acad. Sci. USA*, **100**, 9055–9060.

Spurr, A.R. (1969) A low viscosity epoxy resin embedding medium for electron microscopy. *J. Ultrastr. Res.* **26**, 31–43.

Stadler, L.J. (1940) Gene list and linkage map of corn (maize). *Maize Genet. Coop. Newslett.* **14**, 26–27.

Stinard, P.S., Robertson, D.S. and Schnable, P.S. (1993) Genetic isolation, cloning and analysis of a *Mutator*-induced, dominant antimorph of the maize *amylose extender* locus. *Plant Cell*, **5**, 1555–1556.

Suck, R., Zeltz, P., Falk, J., Acker, A., Kössel, H. and Krupinska, K. (1996) Transcriptionally active chromosomes (TACs) of barley chloroplasts contain the α-subunit of plastome-encoded RNA polymerase. *Curr. Genet.* **30**, 515–521.

Thompson, J.D., Gibson, T.J., Plewniak, F., Jeanmougin, F. and Higgins, D.G. (1997) The ClustalX windows interface: flexible strategies for multiple sequence alignment aided by quality analysis tools. *Nucl. Acids Res.* **24**, 4876–4882.

Uptain, S.M., Kane, C.M. and Chamberlin, M.J. (1997) Basic mechanisms of transcript elongation and its regulation. *Annu. Rev. Biochem.* **66**, 117–172.

Wang, B., Jones, D., Kaine, B.P. and Weiss, M.A. (1998) High-resolution structure of an archaeal zinc ribbon defines a general architectural motif in eukaryotic RNA polymerases. *Structure*, **6**, 555–569.

Weisshaar, B., Armstrong, G.A., Block, A., da Costa e Silva, O. and Hahlbrock, K. (1991) Light-inducible and constitutively expressed DNA-binding proteins recognizing a plant promoter element with functional relevance in light responsiveness. *EMBO J.* **10** (7), 1777–1786.

Wienand, U., Sommer, H., Schwarz, Zs. *et al.* (1982) A general method to identify plant structural genes among genomic DNA clones using transposable element-induced mutations. *Mol. Gen. Genet.* **187**, 195–201.

Wienand, U., Weydemann, U., Niesbach-Klösgen, U., Peterson, P.A. and Saedler, H. (1986) Molecular characterisation of the *c2* locus of *Zea mays*, the gene coding for chalcone synthase. *Mol. Gen. Genet.* **203**, 202–207.

Wind, M. and Reines, D. (2000) Transcription elongation factor SII. *Bioessays*, **22**, 327–336.

Nucleotide sequence data available in the DDBJ/EMBL/GenBank databases: *Etched1* gene (AJ507104), *Etched1* mRNA (AJ507105), *Zmzr1* mRNA (AJ507106).

Nucleotide sequence data available in the Third Party Annotation Section of DDBJ/EMBL/GenBank databases: *Amzr1* (BK001743), *Atzr1* (BK001739), *Crzr1* (BK001725), *Hazr1* (BK001722), *Hvzr1* (BK001720), *Lezr1* (BK001724), *Oszr1* (Bk001721), *Tazr1a* (BK001719), *Vvzr1* (BK001723).